Mapping the modification of ring currents induced by cyclopenta-fusion on a naphthalene core

Patrick W. Fowler,*[a] Erich Steiner,[a] Angela Acocella,[a] Leonardus W. Jenneskens*[b] and Remco W. A. Havenith[b]

[a] *School of Chemistry, University of Exeter, Stocker Road, Exeter, UK EX4 4QD. E-mail: PWFowler@ex.ac.uk; Fax: +44 1392 263434; Tel.: +44 1392 263466*

[b] *Debye Institute, Department of Physical Organic Chemistry, Utrecht University, Padualaan 8, 3584 CH Utrecht, The Netherlands. E-mail: jennesk@chem.uu.nl; Fax: +31 30 2534533; Tel.: +31 30 2533128*

Received (in Cambridge, UK) 14th March 2001, Accepted 16th May 2001
First published as an Advance Article on the web 13th June 2001

An analysis of the σ-, π- and total current density maps, calculated using a distributed-origin coupled Hartree–Fock method, of the non-alternant cyclopenta-fused polycyclic aromatic hydrocarbons (CP-PAH) acenaphthylene (**1**), pyracylene (**2**), fluoranthene (**3**) and cyclopenta[*cd*]fluoranthene (**4**) shows that, whereas the presence of a single pentagon in **1** and **3** has only minor effects on the core naphthalene unit, the strong cooperative effect of the two pentagons connected by a formal double bond in **2** and **4** results in intense paratropic currents in the pentagons, and markedly reduced aromaticity according to conventional criteria. The accuracy of the all-electron maps is supported by calculation of ^{1}H and ^{13}C NMR chemical shifts in agreement with experiment and their interpretation is consistent with nucleus-independent chemical shifts (NICS values). It is shown that the pattern of paratropic contributions can be explained qualitatively within Hückel–London π-electron theory.

Introduction

Externally cyclopenta-fused polycyclic aromatic hydrocarbons (CP-PAH) are of interest in many scientific areas.[1] Representatives of the class have been identified or proposed as ubiquitous combustion products, of which many possess genotoxic activity.[2] CP-PAH are also topical as sub-structures of fullerenes. Furthermore, as a consequence of their non-alternant character,[3] CP-PAH exhibit unusual physico-chemical properties: photophysical properties such as anomalous fluorescence,[4] UV/vis spectra strongly modulated by the distribution and number of pentagons,[5,6] high electron affinities[7,8] and characteristic up-field shifted ^{1}H NMR chemical shifts.[5,6,9] Theoretical interest follows from the role of CP-PAH as probes for the magnetic criteria of aromaticity, and they have been extensively investigated from this point of view.[10–14] The aim of the present work is to provide a direct visualisation of the behaviour of the electrons in these molecules under applied magnetic fields, allowing interpretation of the effects of fusion of five-membered rings on a naphthalene core.

Induced current densities are calculated here and mapped using a proven theoretical method for the family of related molecules [acenaphthylene (**1**), pyracylene (**2**),[15] fluoranthene (**3**) and cyclopenta[*cd*]fluoranthene (**4**)[5,16,17]], all of which contain the naphthalene motif, in order to reveal the nature of the ring currents and relate them to the observed NMR isotropic ^{1}H and ^{13}C chemical shifts.

Ring currents are, of course, not directly observable, though their existence has been inferred in many molecules through their manifestation in NMR and magnetic measurements. The ability to sustain a diatropic current is one criterion of aromaticity,[18] but the observables from which such currents are deduced (^{1}H NMR chemical shifts, magnetic anisotropy, exaltation of diamagnetism) are integrated properties, which may mask local features of the current density. More detailed information is given by, for example, the nucleus-independent chemical shift (NICS) approach,[19] which resolves distinct ring contributions in polycyclic systems, again as integrals with contributions in principle from the whole current density. At a finer level of detail, the currents themselves are important guides to understanding the molecular origins of diatropicity and paratropicity.

Accurate distributed-origin methods for the calculation of the magnetic properties of molecules have been developed in recent years.[20–29] Their efficacy for the computation of electron current densities has been demonstrated for a number of families of conjugated π systems.[30–36] Their particular virtue is that they give a direct visualisation of the current map, which can be checked for reliability by its integration to give magnetic response properties.

Once reliable maps are available, it is often possible to interpret them with simple concepts. In the present case, and perhaps surprisingly, simple Hückel–London π-electron theory[10] turns out to provide a useful guide to the qualitative changes as each molecule is built up around its naphthalene core.

Computational methods

Magnetic properties

Magnetic properties of compounds **1** to **4** were computed using a distributed-origin method at the coupled Hartree–Fock level of theory with the Exeter version of SYSMO[37] in a 6-31G** basis. Molecular geometries were optimised in the 6-31G basis with GAMESS-UK.[38] Basis sets 6-31G, 6-31G* and 6-31G** give essentially identical optimised geometries for these systems (*e.g.*, **1**,[39] **2**[11,33,40]). For current density maps, well converged results are given by the CTOCD (continuous transformation of origin of current density) method in the DZ (diamagnetic zero) variant.[24,25] Its key feature is that it is a distributed method, the current density $\boldsymbol{j}(\boldsymbol{r})$ at any point in space being calculated with that point as origin, giving superior convergence with basis size, and achieving physically realistic current maps with modest basis sets.[26,27]

Two properties derived by integration are the molecular magnetisability ξ, which describes the linear response of the molecular magnetic dipole moment to an applied magnetic

 DOI: 10.1039/b102413m

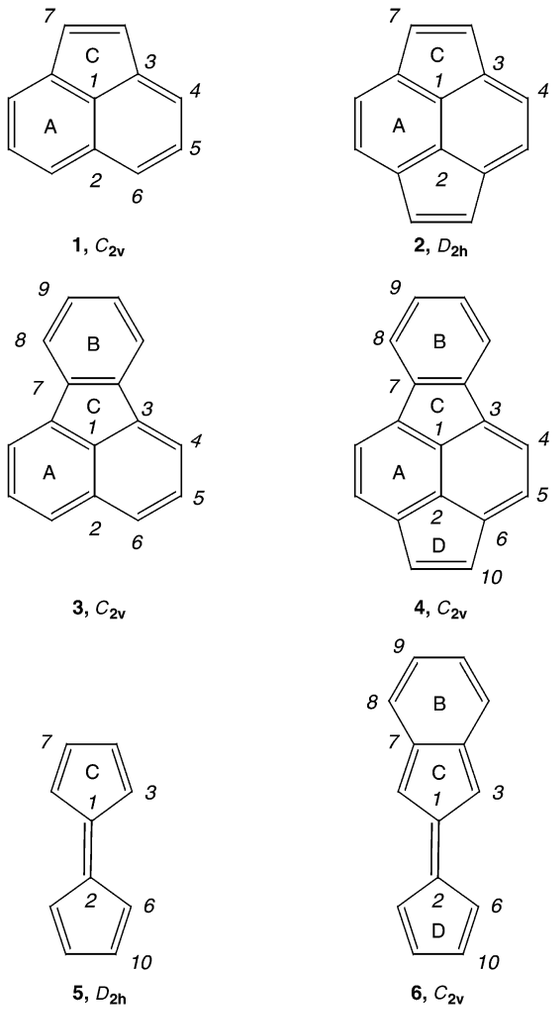

Chart 1 Compounds under investigation, showing generalised atom numbering scheme and depicting by the capitals A–D the geometric centres of the pentagons and hexagons (see text).

field, and the nuclear magnetic shieldings σ, which describe the linear response of the local magnetic field at nuclei to the applied field. Whereas CTOCD-DZ gives satisfactory current maps, it has been established that a PZ2 (paramagnetic zero) variant of the CTOCD method gives more accurate and better converged results for the integrated properties.[29] This is the method used here.

The current densities induced by a magnetic field of unit strength ($\hbar/ea_0^2$) perpendicular to the molecular plane are mapped for each molecule. For a field pointing out of the page, an induced diamagnetic (paramagnetic) circulation of electrons is anticlockwise (clockwise). Electron current densities are computed in a plane 1 a_0 above the nuclei, and hence close to the maximum in the π electron density. The plotting area is a square of side 24 a_0. The contours show the modulus of the complete current density, $|\boldsymbol{j}|$, with contour values 0.001×4^n au, for $n = 0, 1, 2, \ldots$ (the atomic unit of current density, charge density × velocity, is $e\hbar/m_e a_0^4$). The vectors are centred on the points of a 36 × 36 grid, and show the in-plane projection of $\boldsymbol{j}$. At this height above the plane of nuclei the flow is essentially parallel to the molecular plane.

Results and discussion

Geometries

In Fig. 1, salient features of the 6-31G optimised geometries of **1** (C_{2v}), **2** (D_{2h}), **3** (C_{2v}) and **4** (C_{2v}) are reported and compared with available experimental data. Note that the atom numbering deviates from the official IUPAC scheme (see Chart 1). Direct comparison between the computed and experimental geometrical parameters [neutron diffraction (for **1**)[41] and single-crystal X-ray structure analysis (for **2**–**4**)[42–44]] shows good agreement. An exception is the difference between the computed and experimental lengths of the internal naphthalenic carbon–carbon bond [C(1)–C(2)] in **2** and **4**. In the latter compounds, which consist of naphthalenic cores with two externally fused cyclopenta moieties, the computed bond length is systematically shortened (6-31G: **2**, 1.338 Å and **4**, 1.342 Å; experimental: **2**, 1.360 Å and **4**, 1.354 Å). This tendency has been noted previously for **2**.[31] In contrast, for **1** and **3**, which contain only one externally fused pentagon, the corresponding computed and experimental bond lengths are in satisfactory agreement.

It should be kept in mind, however, that comparison between computed and experimental geometries of **1**–**4** is hampered by various factors. For example, single-crystal X-ray structure analysis of **1** at 80 K revealed the presence of three crystallographically independent molecules with poorly defined individual geometries. Only by constrained refinement was a single common molecular geometry obtained.[41] Although the naphthalenic part of the resulting geometry was in agreement with those from X-ray structures of two acenaphthylene derivatives,[45,46] significant differences were found for the double bond [C(7)–C(7′)] of the external five-membered ring (**1**: 1.395 Å; derivatives: 1.363 Å), suggesting a problem with the value derived from experiment for **1**. Similarly, in the case of fluoranthene (**3**) comparison between geometries is complicated by the presence of two crystallographically independent molecules in the solid-state. Furthermore, fluoranthene (**3**)[43] and cyclopenta[*cd*]fluoranthene (**4**)[44] possess non-planar geometries in the solid-state. It follows that the computed geometrical parameters of **1**, **3** and **4** can only be compared with averaged experimental values. Nevertheless, the number of pentagons externally fused to the naphthalenic core correlates with distinct changes of geometrical parameters. Several trends are discernible from comparisons of results within the pairs **1** and **2**, **3** and **4**, respectively: *e.g.*, on introduction of the second fused pentagon (i) the internal naphthalenic C(1)–C(2) bond contracts by 0.02–0.03 Å; (ii) the outer bond C(4)–C(5) of the naphthalenic unit lengthens by *ca.* 0.02 Å, and C(1)–C(3) and C(3)–C(4) expand and contract, respectively, by *ca.* 0.01 Å; (iii) the valence angle C(3)–C(1)–C(3′) widens by *ca.* 4°.

Magnetic properties

The current density maps of **1** to **4** in the chosen plane are given in Figs. 2–5. They show (a) the π, and (b) the total (σ + π) distribution of induced current density.

The σ contribution to the density is not shown explicitly here, as for these molecules maps of σ current show all the usual features of such maps for polycyclic systems. In a σ map, the intense diamagnetic current density around the nuclei would be invisible at this distance above the molecular plane, and the maps would exhibit distributions characteristic of localised covalent bonds, where each σ bond is a centre of diamagnetic circulation and, as a consequence, there is a cumulative paramagnetic σ circulation around the centre of each ring.[30,47,48] The regularity and localised nature of the σ map, though chemically uninformative, are important as indicators of the reliability of the CTOCD method.

In the π maps, distinct regions of both diamagnetic and paramagnetic circulation are visible, and correlate with elements of geometric and electronic structure. The π maps show that in the case of acenaphthylene (**1**, Fig. 2) and fluoranthene (**3**, Fig. 4), with single cyclopenta-fusions, the naphthalene unit is still prominent. The π electron current density on the five-membered ring of **1** is a relatively weak feature that is mainly a localised diamagnetic circulation on the outer double bond, plus some paramagnetic circulation over the five ring carbons.

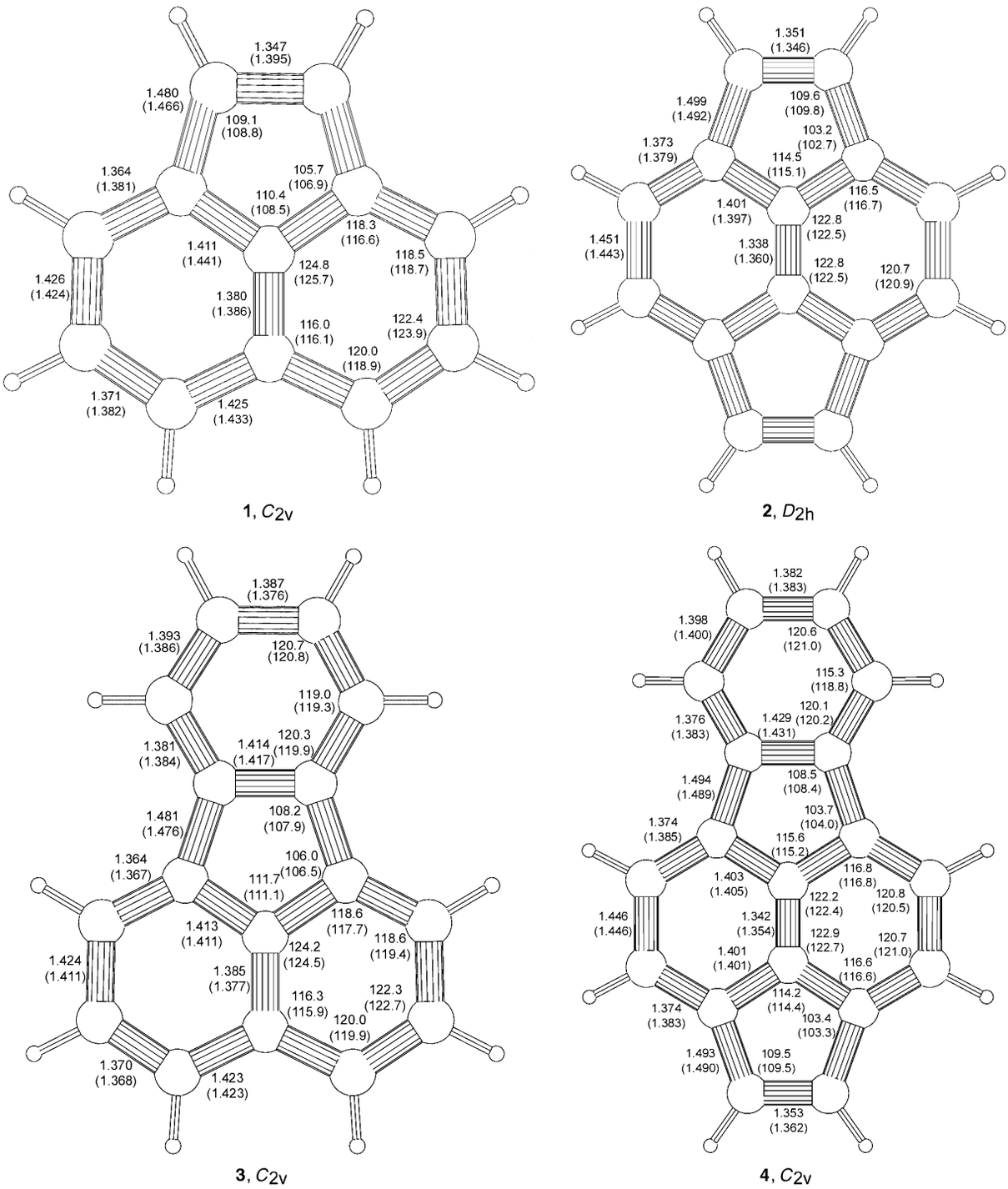

Fig. 1 Computed and experimental (in parentheses) geometrical parameters for **1**–**4**.

In **3**, the π circulation in the five-membered ring is swept away by the strong current of the extra annulated benzenoid six-membered ring, and the molecule appears as a perfect example of two linked classical Hückel systems, the naphthalenic and benzenoid moieties. In both **1** and **3**, the formal non-alternancy[3] of the molecule has negligible effect on the ring-current map: both π current maps break up into *disjoint* alternant regions ($2\pi + 10\pi$ in **1** and $6\pi + 10\pi$ in **3**). The total ($\sigma + \pi$) maps show the same main features, with some increase in the interaction between the alternant fragments coming from the σ electrons, enhancing the paratropicity of the pentagonal rings.

In contrast, the naphthalenic ring current seen in **1** and **3** shows signs of breaking down on addition of a second five-membered ring to **1** and **3**, giving **2** and **4**, respectively (Figs. 3 and 5). In these maps, the five-membered rings have become strong paramagnetic units at the expense of the outer regions of the naphthalene perimeter, and of the attached benzene unit in **4**. In addition, there is a more localised π current on the central double bond of the naphthalene unit in **2** and **4**. The tendency to localisation of the central bond suggests a role for fulvalene-like substructures in the rationalisation of the magnetic properties of these molecules. We will return to this point in the section "Concluding remarks". Nevertheless, as shown previously[11] for **2**, the naphthalenic moiety remains well defined in **2** and **4** and is clearly diatropic.

NICS calculations

The differences in currents observed for pentagonal and hexagonal rings within and between molecules **1** to **4** will be reflected in the central shieldings, *i.e.* the mean $\boldsymbol{\sigma}$ values com-

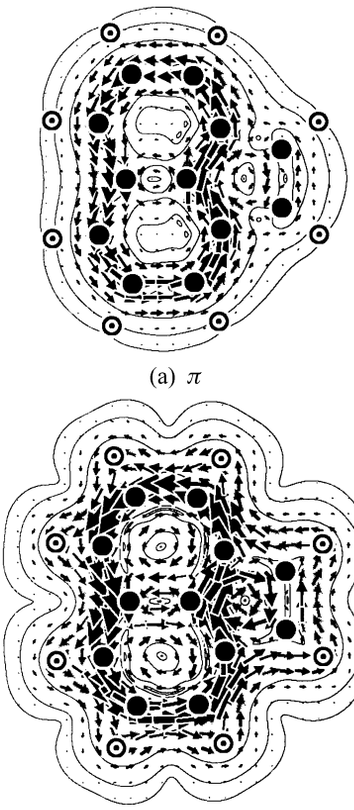

(a) π

(b) $(\sigma + \pi)$

Fig. 2 Current density maps in acenaphthylene (**1**): (a) π current, (b) total (σ + π) current.

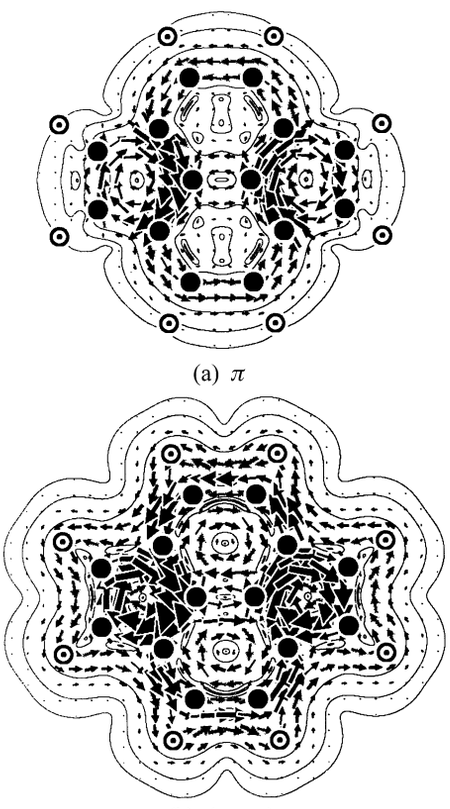

(a) π

(b) $(\sigma + \pi)$

Fig. 3 Current density maps in pyracylene (**2**): (a) π current, (b) total (σ + π) current.

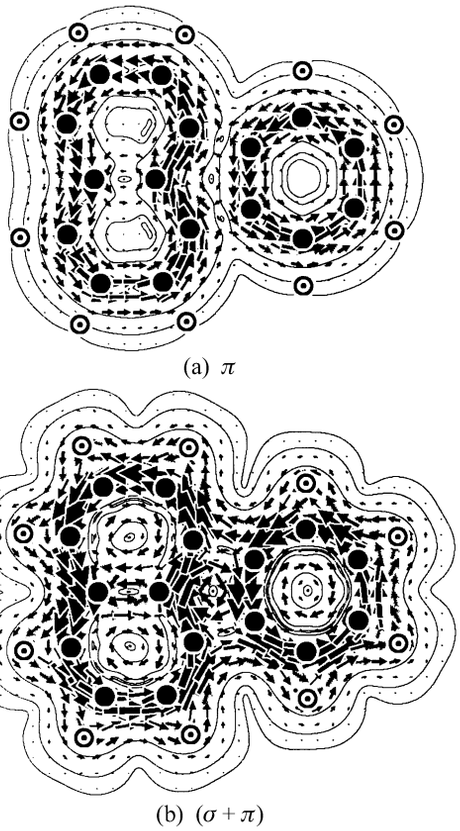

(a) π

(b) $(\sigma + \pi)$

Fig. 4 Current density maps in fluoranthene (**3**): (a) π current, (b) total (σ + π) current.

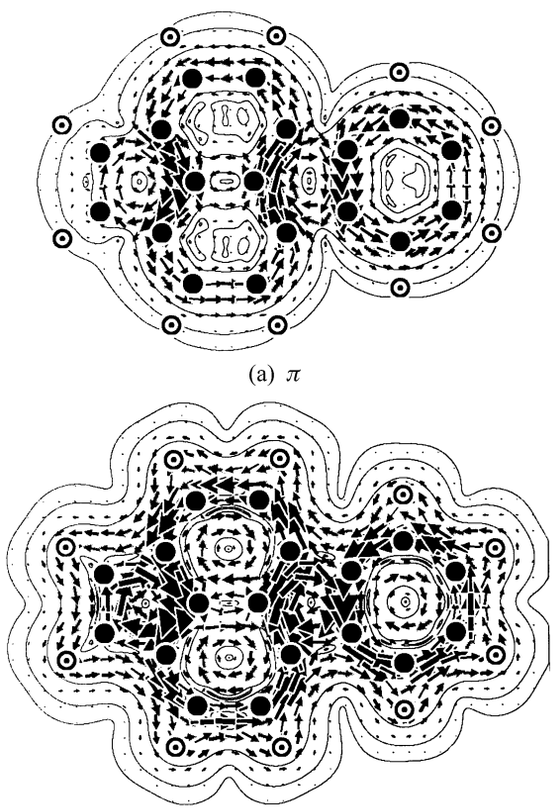

(a) π

(b) $(\sigma + \pi)$

Fig. 5 Current density maps in cyclopenta[*cd*]fluoranthene (**4**): (a) π current, (b) total (σ + π) current.

puted at the respective ring centres. These shielding tensors $\boldsymbol{\sigma}$, apart from sign, represent the NICS values, proposed as indicators of aromatic character.[19] A positive sign for the shielding at the centre of a ring, *i.e.* a negative NICS value, is an indicator of aromaticity. Table 1 shows absolute shielding constants computed at the geometric centres of the symmetry-distinct

Table 1 Computed absolute shielding constants σ (in ppm) at distinct ring centres for **1**–**4**[a]

Compound	Type	σ(out)	σ(in)	$\boldsymbol{\sigma}$
Benzene	A	16.3	10.9	12.7
Naphthalene	A	14.9	12.1	13.1
Acenaphthylene (**1**)	A	10.3	11.9	11.4
	C	−34.3	12.9	−2.9
Pyracylene (**2**)	A	−4.5	13.0	7.2
	C	−56.5	12.4	−10.6
Fluoranthene (**3**)	A	9.9	12.1	11.3
	B	9.4	11.7	10.9
	C	−38.0	14.3	−3.1
Cyclopenta[*cd*]fluoranthene (**4**)	A	−1.2	15.3	9.8
	B	4.6	11.8	9.4
	C	−51.7	13.9	−8.0
	D	−48.9	12.6	−7.9

[a] σ(out) is the component of the absolute shielding out of the plane of the ring, σ(in) is the mean in-plane shielding, and $\boldsymbol{\sigma}$ is the overall mean value. Values calculated in the same way for benzene and naphthalene are included for reference. See Chart 1 for definitions of the hexagon and pentagon type labels.

Table 2 Computed molecular magnetisabilities ξ of **1**–**4**[a]

Compound	ξ(out)	ξ(in)	$\boldsymbol{\xi}$	$\Delta\xi$	Λ
Benzene	−21.3	−4.8	−10.3	−16.5	13.7
Naphthalene	−38.1	−7.6	−17.8	−30.5	30.5
Acenaphthylene (**1**)	−42.2	−8.6	−19.8	−33.6	39.3
Pyracylene (**2**)	−32.7	−9.7	−17.3	−23.0	[b]
Fluoranthene (**3**)	−56.9	−11.8	−26.9	−45.1	42.5
Cyclopenta[*cd*]-fluoranthene (**4**)	−50.7	−12.7	−25.4	−38.8	[b]

[a] ξ(out) is the component of magnetisability out of the plane of the molecule, ξ(in) is the mean in the plane, $\boldsymbol{\xi}$ the overall mean value and $\Delta\xi = \xi(\text{out}) - \xi(\text{in})$ is the anisotropy. Λ is the exaltation.[50] Magnetisabilities are given in atomic units: 1 a.u. = $e^2a_0^2/m_e = 7.89104 \times 10^{-29}$ J T^{-2}. Λ is quoted, as is conventional, in units of 10^{-6} cm^3 mol^{-1}. [b] Values not available.

rings in **1** to **4** at the PZ2 level (Chart 1, hexagons A, B and pentagons C and D, respectively).

The listed mean $\boldsymbol{\sigma}$ values are consistent with the maps, each hexagon having a positive shielding similar to that of benzene and the hexagons of naphthalene (*cf.* Table 1), and each pentagon having a negative shielding. Decomposition of the mean $\boldsymbol{\sigma}$ values into *in-plane* and *out-of-plane* contributions highlights the importance of the mobile π electrons. Whereas the mean in-plane shieldings, σ(in), of both hexagons and pentagons are roughly constant and of positive (diamagnetic) sign, the out-of-plane component, σ(out), clearly distinguishes hexagons and pentagons. All pentagons show large negative (paramagnetic) central shieldings. Hexagons in **1** and **3** have the typical positive sign for σ(out), but those hexagons with two adjacent pentagons in **2** and **4**, for which the maps do indicate a weakening of the naphthalenic unit, are mildly paratropic as measured by their central shieldings. In addition, the independent benzenoid ring of **4** (B) shows a weakened diamagnetism. It has been noted in other cases that tensor components of NICS give a sharper characterisation of the distinction between rings carrying diatropic and paratropic local currents in polycyclic compounds;[14] another strategy has been to take isotropic NICS values but to compute them at out-of-plane positions above the ring centre.[49]

Magnetisabilities

Table 2 lists the computed mean magnetisabilities for ξ molecules **1** to **4**. Magnetisabilities are measures both of the mobility of the electrons in the presence of an external magnetic field and of the size of the region in which the electrons circulate. In fact, on going from **1** to **2** and **3** to **4**, slight falls in magnitude of the mean values $|\boldsymbol{\xi}|$ are found. Tensor component analysis again shows more clearly the influence of paratropic π currents, with the magnitude of $|\xi(\text{out})|$ falling from **1** to **2** and **3** to **4**, despite increasing molecular area and π electron count.

Although formally different quantities, $\Delta\xi = \xi(\text{out}) - \xi(\text{in})$ (computed anisotropy) and Λ (empirical exaltation of isotropic susceptibility),[50] have been found to correlate for a number of polycyclic systems.[14] This correlation holds for the available exaltations listed in Table 2; it is reasonable to suppose that the calculated values of $\Delta\xi = \xi(\text{out}) - \xi(\text{in})$ for **2** and **4** indicate decreased aromaticity for these molecules compared to their relatives **1** and **3**, respectively.

Chemical shifts

Computed ^{1}H and ^{13}C absolute nuclear shielding constants and derived chemical shifts are listed in Tables 3 and 4, where they are compared with experimental shifts. The level of agreement, given the modest basis sets, is satisfactory. The computed ^{1}H NMR chemical shifts (Table 3) all lie within *ca.* 0.5 ppm of the experimental values. For the ^{13}C NMR chemical shifts (Table 4), which of course span a wider range, the deviations between the computed and experimental values are sufficiently small to make the computation a material aid to assignment in most cases. To an extent, this level of agreement is a fortunate consequence of the combination of basis set and the CTOCD method, as results for ^{13}C shifts in the 6-31G** basis can sometimes be closer to experiment than 'accurate' Hartree–Fock limiting results.[27] The deviations from experiment are most significant for the nuclei that belong to five-membered rings in **1**, **2** and **4**.

The proton shifts illustrate the progressive changes in the ring currents within the naphthalene sub-unit. Proton sites 4 in **1**, **2**, **3** and **4** probe the current density on the outer perimeter: whereas the shifts in **1** and **3** (δ = 7.3 and 7.4, respectively) are within 0.3 ppm of the shift δ = 7.6 calculated for naphthalene, the smaller shifts in **2** and **4** (δ = 6.4 and 6.8, respectively) reflect the reduced deshielding effect of the weaker diamagnetic π current. Proton sites 7 in **1** and **2** and 10 in **4** (δ = 6.8, 6.1 and 6.4, respectively) probe the currents in pentagonal rings: the increased shielding in **2** and **4** is now due to the stronger shielding effect of the stronger local paramagnetic π current in the five-membered ring.

All the carbon sites in the CP-PAH molecules have a large, diamagnetic, out-of-plane shielding component, σ(out), and approximately cancelling in-plane principal components that leave a relatively small, usually paramagnetic, in-plane average σ(in). Similar patterns have been observed in individual gauge for different localised orbitals (IGLO) calculations on benzene.[51]

Concluding remarks

The *ab initio* ring current maps for this family of molecules expose a strong co-operative effect between pentagons connected *via* a formal double bond. As a consequence, compounds **2** and **4** have a markedly reduced aromaticity according to the conventional magnetic criteria, which is explained by the large paratropic currents seen in the maps.

Could these currents have been expected on the basis of an intuitive chemical model? One simple approach is to use Hückel π-electron theory in conjunction with the London model, as exploited by Coulson and Mallion[10] and, more recently, by Haddon and co-workers for C_{60}, C_{70} and pyracylene (**2**).[52] Sets of π bond currents computed according to a finite-perturbation, matrix-diagonalisation procedure[52,53] give the results shown in Fig. 6. The calculations used the 6-31G *ab initio* geometries scaled to an average bond length of 1.4 Å for calibration

Table 3 Computed absolute hydrogen (^{1}H) nuclear shielding constants (in ppm) in **1**–**4**[a]

Compound	Nucleus	σ(out)	σ(in)	$\boldsymbol{\sigma}$	δ	Exp[b]
Benzene		21.3	24.7	23.5	7.3	7.3
Naphthalene	3	20.3	25.1	23.5	7.3	7.8
	4	18.9	25.5	23.3	7.6	7.5
Acenaphthylene (**1**)	4	19.6	25.6	23.6	7.3	7.7
	5	20.0	25.0	23.3	7.5	7.6
	6	19.6	25.3	23.4	7.4	7.8
	7	21.9	25.0	24.0	6.8	7.1
Pyracylene (**2**)	4	21.9	25.6	24.4	6.4	6.6
	7	24.3	24.9	24.7	6.1	6.1
Fluoranthene (**3**)	4	18.2	26.0	23.4	7.4	7.9
	5	19.2	25.1	23.1	7.7	7.7
	6	19.0	25.4	23.3	7.5	8.0
	8	18.6	25.9	23.4	7.4	7.9
	9	20.6	24.9	23.5	7.3	7.2
Cyclopenta[*cd*]fluoranthene (**4**)	4	19.9	26.0	24.0	6.8	7.2
	5	20.4	25.6	23.9	6.9	7.1
	8	20.0	25.8	23.9	6.9	7.4
	9	21.5	24.9	23.8	7.0	7.0
	10	23.2	24.9	24.6	6.4	6.5

[a] σ(out) is the component of the absolute shielding out of the plane of the ring, σ(in) is the mean shielding in the plane, and $\boldsymbol{\sigma}$ the overall mean value. Also given are the corresponding δ values, obtained by the rule $\boldsymbol{\sigma} \times 10^6 + \delta = 30.8$.[27] Hydrogen *n* is attached to carbon *n* (see Chart 1). [b] Experimental ^{1}H NMR value (solvent $CDCl_3$).

Table 4 Computed absolute carbon (^{13}C) nuclear shielding constants (in ppm) for **1**–**4**[a]

Compound	Nucleus	σ(out)	σ(in)	$\boldsymbol{\sigma}$	δ	Exp[b]
Benzene		190.8	−8.4	58.0	127.6	128.5
Naphthalene	1	198.0	−20.8	52.1	133.5	133.3
	3	175.0	−1.0	57.7	127.9	127.7
	4	189.0	−4.1	60.2	125.4	125.6
Acenaphthylene (**1**)	1	183.5	−6.6	56.8	128.8	127.4
	2	198.4	−13.2	57.3	128.3	128.4
	3	159.8	−10.3	46.4	139.2	140.0
	4	184.1	−2.0	60.0	125.6	128.7
	5	185.0	−4.7	58.5	127.1	124.1
	6	179.0	−4.1	57.0	128.6	127.9
	7	152.7	2.3	52.4	133.2	127.4
Pyracylene (**2**)	1	170.2	−0.5	56.4	129.2	131.5
	3	153.8	−11.5	43.6	142.0	142.0
	4	178.9	1.2	60.4	125.2	124.8
	7	146.2	0.7	49.2	136.4	132.4
Fluoranthene (**3**)	1	178.0	−11.5	51.7	133.9	133.0
	2	196.9	−15.2	55.5	130.1	130.7
	3	158.4	−7.2	48.0	137.6	137.7
	4	187.0	3.4	64.6	121.0	122.9
	5	185.2	−6.1	57.7	127.9	128.6
	6	178.0	−2.0	58.0	127.6	127.6
	7	155.8	−11.6	44.2	141.4	140.2
	8	186.7	1.4	63.2	122.4	120.7
	9	187.5	−7.2	57.7	127.9	128.3
Cyclopenta[*cd*]fluoranthene (**4**)	1	170.0	−4.4	53.7	131.9	132.9
	2	174.1	−1.6	57.0	128.6	130.5
	3	156.2	−10.3	45.2	140.4	138.9
	4	181.6	6.0	64.5	121.1	121.2
	5	179.5	−1.7	58.7	126.9	125.8
	6	156.7	−9.9	45.6	140.0	140.6
	7	146.5	−11.7	41.1	144.5	142.8
	8	185.1	0.7	62.1	123.5	123.0
	9	186.5	−7.3	57.3	128.3	128.4
	10	148.0	1.2	50.1	135.5	131.7

[a] Notation as Table 3 (see footnote to Table 3); δ values for ^{13}C are obtained by the rule $\boldsymbol{\sigma} \times 10^6 + \delta = 185.6$.[27] [b] Experimental ^{13}C NMR value (solvent $CDCl_3$).

against a notional benzene π bond current. It is striking that these simple idealisations exhibit the main features of the *ab initio* maps: close-to-disjoint alternant fragments in **1** and **3**, depletion of naphthalenic circulation in **2** and **4**, and co-operative paratropic currents in fulvalene-like pentagon pairs.

What these π-only pictures fail to show in the case of **2** and **4** is the strength of the residual current in the naphthalenic hexagonal rings; they exaggerate the relative strength of the paratropic currents. Nonetheless, at this Hückel–London level of theory the fulvalenic subgraph emerges as a useful predictor of the pentagon behaviour, a localised pattern which would not be picked up by a pure ring-perimeter model.[54,55]

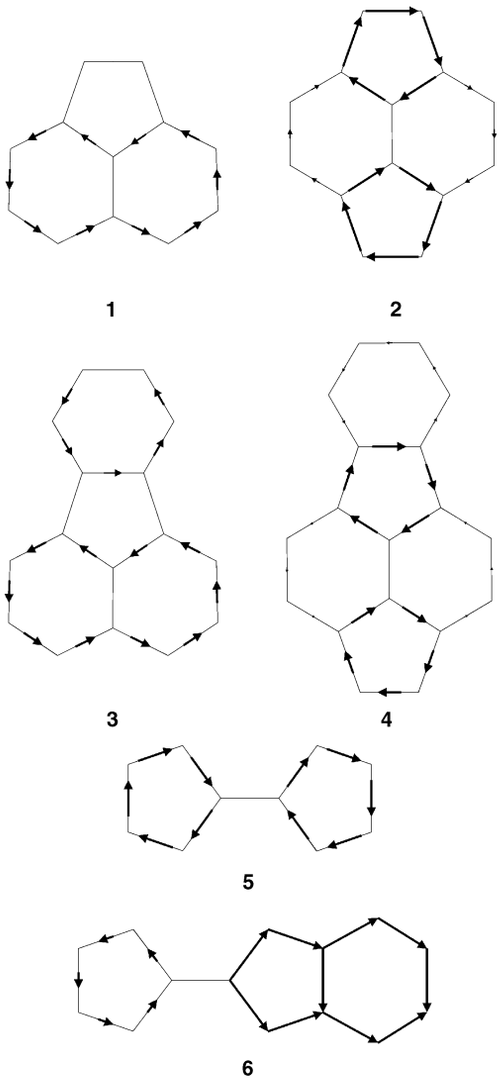

Fig. 6 Schematic Hückel–London π-current density maps in **1**–**6**.

In the Hückel–London model, both fulvalene (**5**) and its derivative **6** when treated as isolated fragments show intense and probably exaggerated paramagnetic circulations in three of the four pentagons, attributable to HOMO–LUMO interaction across the small gaps of these electron-deficient π systems. CTOCD calculation using the same approach as for **1** to **4** points to differences between **5** and **6** as fragments and as hypothetical free molecules.[56] Thus, the fulvalene *molecule* **5** itself and its derivative **6** also show a pattern of paratropic currents (Figs. 7 and 8) when treated by the full CTOCD method of calculation, though these are essentially the usual paratropic ring-centre currents arising from the σ orbitals; at the optimised geometry of the isolated molecule **5** the outer bonds are elongated and the π currents are relatively localised on the formal double bonds of the leading Kekulé structure. In the fulvalenic substructure present in the CP-PAH molecules **2** and **4**, these bonds are shorter, and the π currents delocalise around the pentagons. Similarly, the free molecule **6** has localised π currents that follow the fulvalene–diene Kekulé structure indicated in Chart 1.

Acknowledgements

The authors thank the European Union TMR Network scheme, contract FMRX-CT097-0126 (USEFULL), for financial support, allowing A. A. (University of Bologna) to work for three months in Exeter, the British Council/CW-NWO for a travel grant to P. W. F., E. S. and L. W. J.

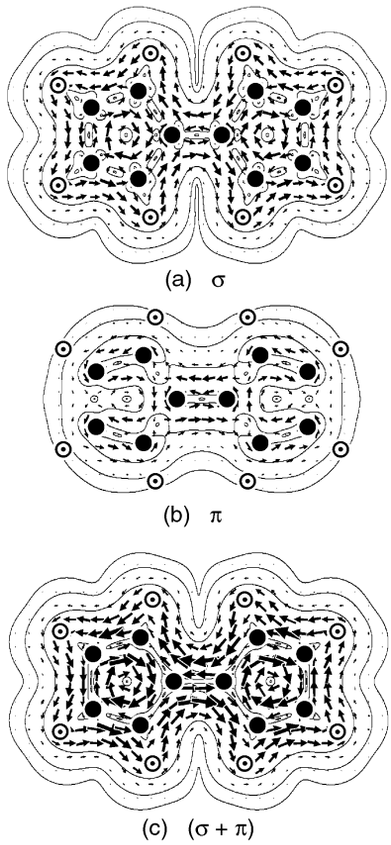

Fig. 7 Current density maps in fulvalene (**5**): (a) σ current, (b) π current, (c) total (σ + π) current.

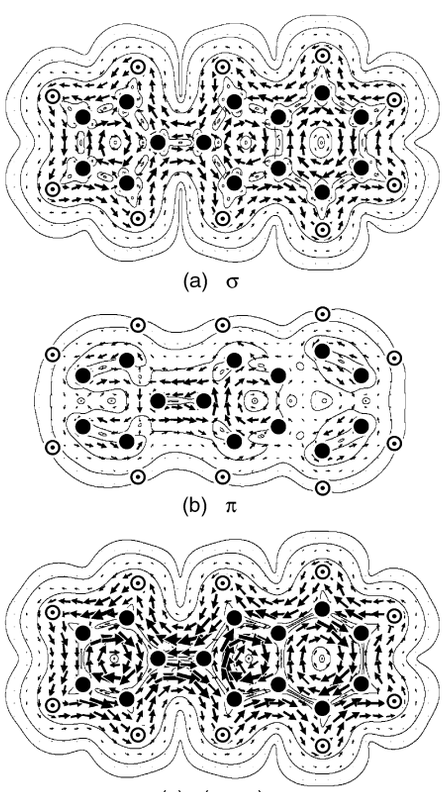

Fig. 8 Current density maps in the fulvalene derivative (**6**): (a) σ current, (b) π current, (c) total (σ + π) current.

References

1 For a review: R. G. Harvey, *Polycyclic Aromatic Hydrocarbons*, Wiley-VCH, New York, 1997.

2 For a review: U. E. Wiersum and L. W. Jenneskens, in *Gas Phase Reactions in Organic Synthesis*, ed. Y. Vallée, Gordon and Breach Science Publishers, Amsterdam, ch. 3, 1997 and references cited therein.
3 A. Streitwieser, Jr., *Molecular Orbital Theory for Organic Chemists*, Wiley, New York, 1967.
4 For example: C. Gooijer, I. Kozin, N. H. Velthorst, M. Sarobe, L. W. Jenneskens and E. J. Vlietstra, *Spectrochim. Acta*, *Part A*, 1998, **54**, 1443 and references cited therein.
5 M. Sarobe, J. D. Snoeijer, L. W. Jenneskens, M. Q. Slagt and J. W. Zwikker, *Tetrahedron Lett.*, 1995, **36**, 8489.
6 M. Sarobe, S. Flink, L. W. Jenneskens, B. L. A. van Poecke and J. W. Zwikker, *J. Chem. Soc.*, *Chem. Commun.*, 1995, 2415.
7 R. C. Haddon, *The Fullerenes: Powerful Carbon-Based Electron Acceptors*, in *The Fullerenes. New Horizons for the Chemistry, Physics and Astrophysics of Carbon*, eds. H. W. Kroto and D. R. M. Walton, Cambridge University Press, Cambridge, UK, 1993, p. 53.
8 M. Sarobe, PhD Thesis, *Polycyclic Aromatic Hydrocarbons under High Temperature Conditions: Consequences for Carbon Build-up during Combustion and Fullerene Formation Processes*, Utrecht University, Utrecht, The Netherlands, 1998, ch. 9.
9 L. T. Scott and A. Necula, *J. Org. Chem.*, 1996, **61**, 386.
10 C. A. Coulson and R. B. Mallion, *J. Am. Chem. Soc.*, 1976, **98**, 592.
11 P. W. Fowler, R. Zanasi, B. Cadioli and E. Steiner, *Chem. Phys. Lett.*, 1996, **251**, 132.
12 G. Subramian, P. v. R. Schleyer and H. Jiao, *Organometallics*, 1997, **16**, 2362 and references cited therein.
13 A. M. Orendt, J. C. Facelli, S. Bai, A. Rai, M. Gossett, L. T. Scott, J. Boerio-Goates, R. J. Pugmire and D. M. Grant, *J. Phys. Chem. A*, 2000, **104**, 149 and references cited therein.
14 P. W. Fowler, E. Steiner and L. W. Jenneskens, *Angew. Chem.*, 2001, **113**, 375; P. W. Fowler, E. Steiner and L. W. Jenneskens, *Angew. Chem.*, *Int. Ed.*, 2001, **40**, 362.
15 M. Sarobe, S. Flink, L. W. Jenneskens, J. W. Zwikker and J. Wesseling, *J. Chem. Soc.*, *Perkin Trans. 2*, 1996, 2125 and references cited therein.
16 L. W. Jenneskens, M. Sarobe and J. W. Zwikker, *Pure Appl. Chem.*, 1996, **68**, 219 and references cited therein.
17 L. T. Scott, *Pure Appl. Chem.*, 1996, **68**, 291 and references cited therein.
18 P. v. R. Schleyer and H. Jiao, *Pure Appl. Chem.*, 1996, **68**, 209 and references cited therein.
19 P. v. R. Schleyer, C. Maerker, A. Dransfeld, H. Jiao and N. J. R. van Eikema Hommes, *J. Am. Chem. Soc.*, 1996, **118**, 6317.
20 T. G. Edwards and R. McWeeny, *Chem. Phys. Lett.*, 1971, **10**, 283.
21 R. Ditchfield, *Mol. Phys.*, 1974, **27**, 789.
22 W. Kutzelnigg, *Isr. J. Chem.*, 1980, **19**, 193.
23 M. Schindler and W. Kutzelnigg, *J. Chem. Phys.*, 1982, **76**, 1919.
24 T. A. Keith and R. F. W. Bader, *Chem. Phys. Lett.*, 1993, **210**, 223.
25 S. Coriani, P. Lazzeretti, M. Malagoli and R. Zanasi, *Theor. Chim. Acta*, 1994, **89**, 181.
26 T. A. Keith and R. F. W. Bader, *J. Chem. Phys.*, 1993, **99**, 3669.
27 R. Zanasi, *J. Chem. Phys.*, 1996, **105**, 1460.
28 P. Lazzeretti, M. Malagoli and R. Zanasi, *Chem. Phys. Lett.*, 1994, **220**, 299.
29 R. Zanasi, P. Lazzeretti, M. Malagoli and F. Piccinini, *J. Chem. Phys.*, 1995, **102**, 7150.
30 E. Steiner and P. W. Fowler, *Int. J. Quantum Chem.*, 1996, **60**, 609.
31 P. W. Fowler and E. Steiner, *J. Phys. Chem. A*, 1997, **101**, 1409.
32 I. Černušák, P. W. Fowler and E. Steiner, *Mol. Phys.*, 1997, **91**, 401.
33 P. W. Fowler, E. Steiner, B. Cadioli and R. Zanasi, *J. Phys. Chem. A*, 1998, **102**, 7297.
34 P. W. Fowler, E. Steiner, R. Zanasi and B. Cadioli, *Mol. Phys.*, 1999, **96**, 1099.
35 I. Černušák, P. W. Fowler and E. Steiner, *Mol. Phys.*, 2000, **98**, 945.
36 A. Ligabue, U. Pincelli, P. Lazzeretti and R. Zanasi, *J. Am. Chem. Soc.*, 1999, **121**, 5513.
37 P. Lazzeretti and R. Zanasi, 1980, SYSMO package (University of Modena, Italy) with additional Exeter routines for evaluation and plotting of current density.
38 M. F. Guest, J. H. van Lenthe, J. Kendrick, K. Schöffel, P. Sherwood and R. J. Harrison, *GAMESS-UK a package of ab initio programs*, 1998. With contributions from R. D. Amos, R. J. Buenker, M. Dupuis, N. C. Handy, I. H. Hillier, P. J. Knowles, V. Bonacic-Koutecky, W. von Niessen, V. R. Saunders and A. J. Stone. It is derived from the original GAMESS code due to M. Dupuis, D. Spangler and J. Wendolowski, NRCC Software Catalog, Vol. 1, Program No. QG0 (GAMESS) 1980.
39 R. C. Peck, J. L. Schulman and R. L. Disch, *J. Phys. Chem.*, 1990, **94**, 6637.
40 J. L. Schulman and R. L. Disch, *J. Mol. Struct.* (*THEOCHEM*), 1992, **259**, 173.
41 R. A. Wood, R. Welberry and A. David Rae, *J. Chem. Soc.*, *Perkin Trans. 2*, 1985, 451.
42 B. Freiermuth, S. Gerber, A. Riesen, J. Wirz and M. Zehnder, *J. Am. Chem. Soc.*, 1990, **112**, 738.
43 A. C. Hazell, D. W. Jones and J. M. Sowden, *Acta Crystallogr.*, *Sect. B: Struct. Crystallogr. Cryst. Chem.*, 1977, **33**, 1516.
44 M. Lutz, A. L. Spek, M. Sarobe and L. W. Jenneskens, *Acta Crystallogr.*, *Sect. C: Cryst. Struct. Commun.*, 1999, **55**, 659.
45 H. Bouas-Laurent, M. Desvergne, J. Gaultier and C. Hauw, *Cryst. Struct. Commun.*, 1973, **2**, 547.
46 K. Harano, M. Yasuda and K. Kanematsu, *Cryst. Struct. Commun.*, 1981, **10**, 209.
47 P. Lazzeretti and R. Zanasi, *Chem. Phys. Lett.*, 1981, **80**, 533.
48 P. Lazzeretti, E. Rossi and R. Zanasi, *Nuovo Cimento Soc. Ital. Fis.*, *D*, 1982, **1**, 70.
49 For example: P. v. R. Schleyer, H. Jiao, N. J. R. van Eikema Hommes, V. G. Malkin and O. L. Malkina, *J. Am. Chem. Soc.*, 1997, **119**, 12669.
50 H. J. Dauben, J. D. Wilson and J. L. Laity, *Diamagnetic Susceptibility Exaltation as a Criterion of Aromaticity In Nonbenzenoid Aromatics*, vol. II, ed. J. P. Snyder, Academic Press, New York, 1971.
51 U. Fleischer, W. Kutzelnigg, P. Lazzeretti and V. Mühlenkamp, *J. Am. Chem. Soc.*, 1994, **116**, 5298 and references cited therein.
52 A. Pasquarello, M. Schlüter and R. C. Haddon, *Phys. Rev. A*, 1993, **47**, 1783.
53 A. Ceulemans, L. F. Chibotaru and P. W. Fowler, *Phys. Rev. Lett.*, 1998, **80**, 1861.
54 J. R. Platt, *J. Chem. Phys.*, 1954, **22**, 1448.
55 For a recent application of the ring perimeter model on several CP-PAH see: M. Kataoka, *Tetrahedron*, 1997, **53**, 12875.
56 For recent *ab initio* calculations on the unknown **5**: A. P. Scott, I. Agranat, P. U. Biedermann, N. V. Riggs and L. Radom, *J. Org. Chem.*, 1997, **62**, 2026.